Chapter 6

Data Reduction and Analysis

The sections of this chapter can be split into three categories. The first category is the filtering of data and the creation of neutral DSTs. Two sections describing the offline code that pertains to the central calorimeter are the second category. The last category is the cuts involved in candidate event selection.

6.1 Filtering

After a data run has ended, the data tape is transferred to a tape drive on one of the E760 workstations; a program[1] is run using the data tape as input. This program serves several purposes; the data is filtered and split into several data sets, statistics for all detectors are generated and a preliminary analysis of charged events is done.

Events from both of the two charged physics triggers (MLU1 and MLU2) are selected and written to separate data files[2]. The MLU1 events are also subject to

[1]The program is entitled DO_DST. Although DST is part of the program's name, only filtering is done; no data summary is done at this level.

[2]The files are labelled RUN#_MLU1.DST and RUN#_MLU2.DST, respectively.

analysis producing a very preliminary charmonium data sample based upon the easily identified inclusive J/ψ decays (equation 1.3). This has been very useful for a quick count of candidate events when a resonance is being scanned with one stack; this has not been applicable during the $^1P_1$ search.

A similar file[3] is made for neutral events except an event selection based upon the ACP3 software trigger bits is done; the ACP3 software trigger bits were described in table 5.6. For an event to be written to this file, one of the following sets of requirements is met:

- there exists an invariant mass ≥ 2.0 GeV/c^2 in the event,
- the two largest energy deposits satisfy two body kinematics for $\gamma\gamma$ events,
- there are more than two clusters and one pair of clusters results in an invariant mass[4] that is associated with a π^o, or
- the number of clusters is ≥ 6 and two η invariant masses are formed by four clusters[5]

A calibration file is made with further cuts involving the filtered neutral events to select all $\bar{p}p \rightarrow \pi^o\pi^o$. Within a stack, the calibration files are combined into one

[3]The file name is RUN#_MLU4.DST.

[4]Neither of the two clusters can be used with a different cluster to form a separate acceptable invariant mass (section 5.4).

[5]Same as previous footnote.

file and used to calibrate the entire stack of data (section 4.3.4). The calibration is usually finished within a few days of the end of a stack.

Further filtering of MLU1 and MLU4 events occurs[6]. During the quick analysis of MLU1 events by the filtering program, if there is an invariant mass pair greater than 2.2 GeV/c^2 then the event is written to the file. The events with at least one invariant mass $\geq$ 2.5 GeV/c^2 software bit ON for MLU4 events are written to the other file.

A further filtering of the MLU1 data is performed by doing the following basic analysis. For each energy in a stack, a file[7] is written containing events with two charged particles that satisfy a very loose electron identification with a large invariant mass. The loose electron identification allows for missing Čerenkov detector signals in the septa region.

6.2 Neutral DSTs

The neutral DSTs consist of short summaries for all neutral events. The central calorimeter clustering algorithm and pile-up analysis, which are described in the following sections, are used in making the summaries for the neutral DSTs. The central

[6] The resulting events are written to files labelled RUN#_COM1.DST and RUN#_COM4.DST, respectively.

[7] These files are called MINI DSTs.

calorimeter cluster energy threshold is 25 MeV while 50 MeV is the threshold for a cluster in the forward calorimeter.

A neutral event summary contains information about the formed clusters in both the forward and central calorimeter. For all formed clusters, the position and energy are in the summary as well as a hit map of the counters or modules in a 3×3 grid that are assigned to the cluster (see the next section). The pile-up determinations for the central calorimeter clusters (section 6.4) are included. Also included in each summary is information which uniquely identifies the event, the extra energy in the counters and modules not associated with clusters, and hit maps for the H1, H2 and Čerenkov detectors.

6.3 Clustering

Determining which blocks constitute a particle's energy deposit has been under investigation since the AGS test (section 4.2.1). The basic cluster configuration is a 3×3 grid centered upon the largest energy deposit in an area. The clustering algorithm has evolved to distinguish single electromagnetic shower inducing particles from coalesced gamma rays from symmetric π^o decay.

The original version (and a basic outline of the current version) uses the 3×3 grid and the energy deposit's center of gravity to determine the position of the incident particle. The 3×3 grid of all counters with signals above pedestals is formed around the counter with the highest energy deposit in the hit counter list (or a small section of the calorimeter in the current version of the clustering algorithm). After the counters included in the formed cluster are removed from the hit counter list, another energy deposit is located for clusterization. Clusters are formed until there are no more counters above threshold for the central energy deposit and no 3×3 grid energy above the total cluster energy threshold; this is similar to the ACP program's clustering algorithm (section 5.4).

The current, and better, offline version looks for local energy deposit maxima and forms clusters about the maxima. A single 3×3 cluster is formed about an energy deposit maximum when the nearest maximum is more than 4.25 block units away in any direction; in this case, the energy deposit is considered an isolated cluster.

Each isolated cluster energy deposit position is corrected by using the sum of two exponentials, shower core and tail profiles [77]. The parameterization of the two profiles is determined from studying the e^+e^- energy deposits from data taken at the J/ψ resonance. These energy deposits are also used to study energy loss of the electromagnetic shower due to the stainless steel septa. The cluster energy is corrected for energy loss.

The distances in both ring and wedge units (x_r and x_w, respectively, in units of blocks) between an energy deposit's center of gravity and the center of the central block of a 3×3 grid are used to correct the position of the incident particle. The new position is dependent upon these measured distances and parameterization of the electromagnetic shower. The corrected ring distance from the center of the central

Parameter	Value Ring	Wedge
A	0.2601	0.3138
a	0.0321	0.0397
B	0.2574	0.1969
b	0.1860	0.1715

Table 6.1: The empirically determined parameters for correcting the position of an energy deposit in the central calorimeter, equation 6.1. All paramters are in units of blocks.

block (similarly for the corrected wedge distance) is

$$d_r = A_r(1 - e^{-\frac{x_r}{a_r}}) + B_r(1 - e^{-\frac{x_r}{b_r}}), \tag{6.1}$$

where A, B, a, and b are constants determined empirically from $J/\psi \to e^+e^-$ and d is the same direction from the center of the central block as x. Table 6.1 contains the empirically determined parameters. The corrected position is then translated from the block coordinate system (ring and wedge) to the laboratory system (θ and ϕ).

The electromagnetic shower energy lost in the septa is corrected for by using a parameterization of the shower profile and the position of the incident particle. The distance from the closest ring and wedge edges of the block: y_r and y_w, respectively, where $d_r + y_r = d_w + y_w = \frac{1}{2}$ of a block. The total energy deposited in a 3×3 grid, E_{seen}, is corrected to

$$E_{corr} = \frac{E_{seen}}{(1 - F_{half}e^{-\frac{y_r}{f_{half}}})(1 - G_1e^{-\frac{y_w}{g_1}} - G_2e^{-\frac{y_w}{g_2}})}, \tag{6.2}$$

where F_{half} and f_{half} depend upon which half of the block the particle is incident upon, due to the staggering of blocks in the ring direction, and the two sets of parameters in the wedge direction (G_i and g_i) are due to the two wedge shells separating blocks

Paramter	Value	Paramter	Value
F_{low}	0.0614	G_1	0.1474
f_{low}	0.1357	g_1	0.0204
F_{high}	0.0857	G_2	0.1594
f_{high}	0.0508	g_2	0.0784

Table 6.2: The empirically determined parameters for correcting the energy of an energy deposit in the central calorimeter, equation 6.2. Paramters f and g are in units of blocks while parameters F and G are dimensionless.

in the azimuth. The parameters F_{low} and f_{low} (F_{high} and f_{high}) are used when the determined polar angle θ of the incident particle is less than (greater than) than the θ that corresponds to the center of the central block. The parameters are empirically determined from $J/\psi \rightarrow e^+e^-$ data and are presented in table 6.2.

A cluster mass M_{cl} is formed by taking the counters in a 5×5 grid and forming an invariant mass for the cluster,

$$M_{cl} = \sqrt{\left(\sum_i E_i\right)^2 - \left(\sum_i \vec{p}_i\right)^2} \tag{6.3}$$

where E_i is the energy of the i^{th} counter and $\vec{p}_i = E_i\hat{x}_i$ where $\hat{x}_i$ is the unit vector from the interaction point to the center of the i^{th} counter. A single cluster energy deposit is split into two clusters when the cluster mass is > 100 MeV. A group of counters is also split into two clusters when two energy deposit maxima are separated by less than 4.25 block units.

The two profiles are used when separating two nearby energy deposit maxima or when an isolated energy deposit's cluster mass is > 100 MeV. The energies of the blocks common to both clusters are shared (the assumption being that each deposit is caused by separate electromagnetic showers). The fractions of the energy deposited in a shared counter (a counter that is assigned to the two clusters) is a function of the distance between the shared counter and the two main counters (where the energy deposit maxima are located) and the shower profiles. The determination of the fractions of any shared counter is an iterative process and is complete when the profiles for each shower deposit are satisfied.

The method of splitting energy deposits has succeeded in identifying energy deposits from coalesced π^o decays (see figure 7.5). The clustering algorithm described above assumes all incident particles are electromagnetic shower inducing particles: electrons, positrons or gammas. Hadronic interactions can be punch through particles (see sections 4.3.2 and 4.4.2), have symmetric energy deposits, or asymmetric energy deposits. Since a punch through particle signal is only one counter, the exact position of a punch through cannot be determined and it is nominally positioned at the center of the counter hit. Large signals resulting from hadronic interactions may or may not mimic electromagnetic shower signals. Both symmetric and asymmetric hadronic signals can be split due to the resulting cluster mass or by virtue of having two energy maxima.

6.4 Pile-up

Pile-up is defined to be extraneous signals from interactions, other than the event being triggered upon, nearby in time. The central calorimeter counters' FERA ADCs are gated for 150 ns. Triggered signals are supposed to start 20 ns after the

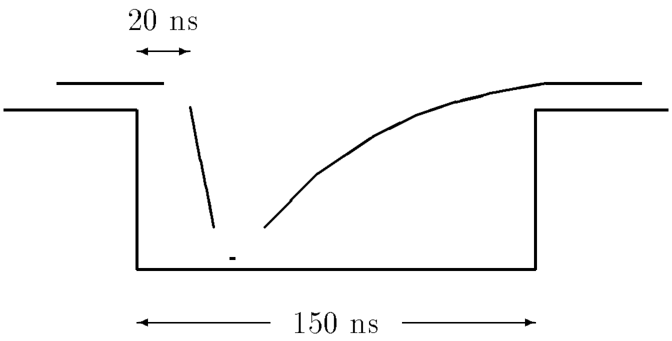

Figure 6.1: A single calorimeter counter signal shown in relationship to the FERA ADC gate.

start of the gate as shown in figure 6.1. Interactions occurring nearby in time cause signals, such as the one shown in figure 6.1, to be shifted in time with respect to the FERA gate. The tail of the signal shown in figure 6.1 is not a good representation; the central calorimeter counter signals are long, with 90% of the charge being collected in 240 ns (an additional 7% of the charge is collected in the following 150 ns). Hence, most pile-up signals come from previous interactions, when tails of earlier large energy deposits are collected within the triggered gate for the central calorimeter.

The data acquisition electronics do not have any timing information for the individual counter signals. However, signals from both the Level I and II summers can be used to identify pile-up signals. Below is a description of the signals available and how they are used to determine whether or not a central calorimeter signal/cluster is caused by the interaction triggered upon. Analysis code determines the extraneous signals as *out-time* clusters as well as identifying the trigger interaction signals as *in-time* clusters. However, there are some signals which can neither be identified as being in-time nor out-time clusters and are classified as *non-determined* clusters.

The Level I signals that are used come from the 160 latches, or pattern units. The 160 discriminated signals, discussed in section 2.9, that form the minimum bias are connected to latch units. The pattern units essentially give a 30 ns *snapshot* about the minimum bias signal for the event (the peak of an in-time signal). During the 1990 data taking run, the discriminator energy threshold was $\approx$ 80 MeV; amplifiers were installed prior to the 1991 data taking run, reducing the effective threshold of the pattern units to $\approx$ 40 MeV. However, the pattern unit thresholds do not necessarily correspond to the cluster energy threshold since a cluster's energy deposit can involve more than one 1×9 set of counters which make up a Level I sum.

The 40 Level II summer discriminators are used for the hardware trigger and set with thresholds which correspond to expected e^+e^- pairs from $\bar{c}c$ decays and are not used for pile-up determination. As discussed in section 2.9, each of the 40 Level II sums is also split into two signals which go to FERA ADC's. The difference between the two recorded signals is that one signal is timed the same as the individual counters signals, ADC_{trigg}, and the other is delayed to look at the energy prior to and/or at the beginning of the trigger, ADC_{delay}. Figure 6.2 shows the three configurations of the ADC_{delay} gate width and delay amount used during the 1990 and 1991 data taking periods. In 1990, the ADC_{delay} gate width was 150 ns; during the first (second) part of data taking in 1990 the delay was 100 ns (150 ns) and the overlap was 50 ns (none), see figure 6.2a (figure 6.2b). After studying both 1990 configurations, it was decided

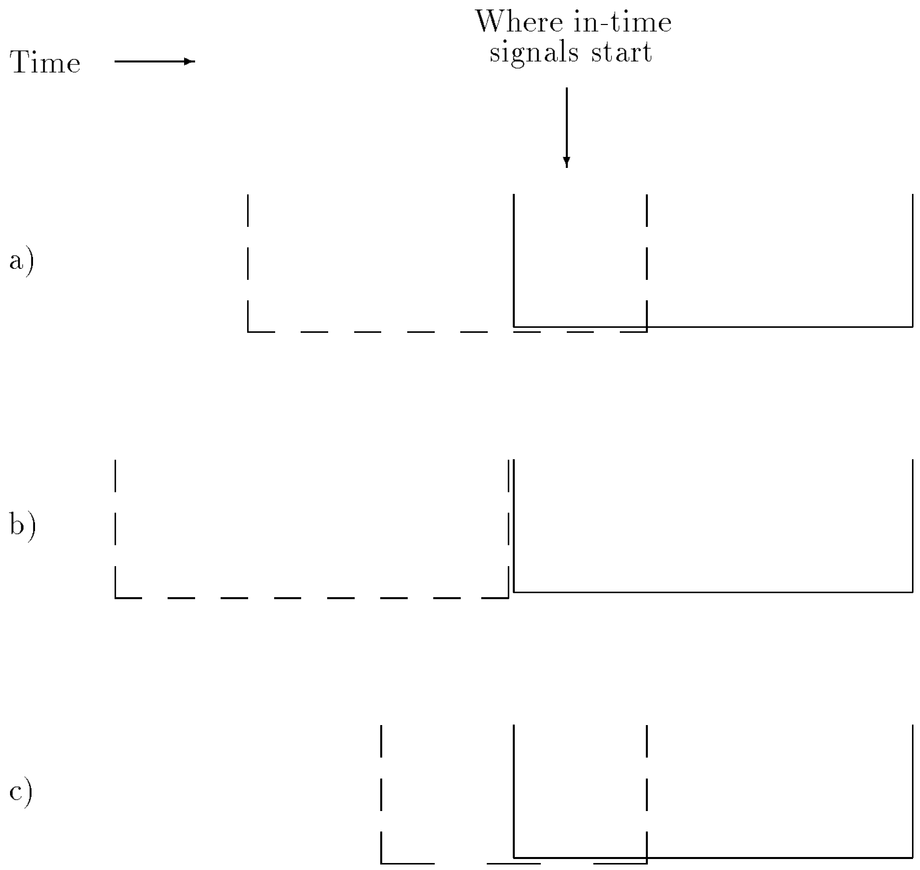

Figure 6.2: The three configurations of overlap of the two Level II summer signals: (a) 1990 overlapped gates, (b) 1990 separated gates, (c) 1991 overlapped gates.

to use an overlap of the two ADC gates of 50 ns and shorten the gate width to 100 ns for the delayed gate thus making the delay amount 50 ns, shown in figure 6.2c.

For all three configurations shown in figure 6.2, a ratio for each super-block is defined as

$$R_{II} = \frac{ADC_{delay}}{ADC_{trigg}}. \tag{6.4}$$

A range of acceptable ratios R_{II} has been determined for each configuration which defines the in-time signals. If the ratio of a super-block is less than the acceptable range, then there is at least one energy deposit in the super block which came after the trigger interaction; the 1990 time separated gates (figure 6.2b) could not distinguish these types of signals. On the other hand, when a super-block's ratio is greater than the range, there is at least one energy deposit which came from an earlier interaction. Note that a super-block can contain more than one cluster; a super-block's ratio is strongly influenced by large energy deposits.

All clusters are initially assumed to be non-determined clusters in the offline pile-up analysis code. There are several possible criteria for determining whether a cluster is an in-time or out-time cluster. If a cluster does not fit any of the in-time or out-time cluster criteria for all the steps, the cluster remains as a non-determined cluster. If during the pile-up analysis a cluster is determined to satisfy criteria of an in-time cluster, it is declared as such and the analysis moves onto the next cluster. When a cluster is determined to be an out-time cluster, it is declared as such and the analysis continues with that cluster. A determined out-time cluster can satisfy the in-time cluster criteria at a later step in the pile-up analysis and be declared an in-time cluster, which would then cause the analysis to move onto the next cluster. Clusters are given every chance to satisfy the in-time cluster criteria.

The pile-up analysis uses the position determined by the clustering algorithm to determine which counter the cluster is centered about. Certain counters are in overlap regions for the Level I and Level II summers; therefore counters can be in 1 or 2 pattern units and 1, 2, or 4 super-blocks. The following are the pile-up analysis steps taken using the 1991 configuration which is the relevant set-up for the $^1P_1$ search.

- The first step checks to see if the cluster is isolated in one of the super-blocks and that the FERA ADCs are above a threshold. The threshold is nearly equivalent to $\approx$ 30 MeV collected by ADC_{trigg} which corresponds to ADC_{delay} being a few counts above pedestal for in-time signals. If a cluster is isolated within a super-block (no other clusters are located in the super-block) and above threshold, either an in-time or out-time determination is made using R_{II}.
- The second step uses the Level I pattern units by comparing the amount of energy deposited by a cluster in a pattern unit, $E_{PU}^{cluster}$, with the summed energy deposited in the 1×9 set of counters of the Level I sum, E_{PU}^{summer}. For each pattern unit that the cluster has deposited energy (three pattern unit 1×9 sets can be affected by a 3×3 grid energy deposit), an in-time cluster determination results when the $E_{PU}^{summer} - E_{PU}^{cluster} < 10$ MeV and the pattern unit is ON; an

out-time cluster determination occurs when $E_{PU}^{cluster} > 50$ MeV and the pattern unit is OFF.

- The third step requires the cluster's energy deposit to be greater than 75% of the total energy deposited in a super-block. When more than one cluster is in a super-block, the larger energy deposit is the main contribution to the super-block's ratio, R_{II}, and therefore the ratio is used to determine the larger energy deposit cluster to be an in-time or out-time cluster.

- The last step uses the super-block's R_{II} when there are two nearly equal energy deposits within a super-block. If both of the two clusters make up between 45% and 55% of the super-block's deposited energy and R_{II} satisfys the in-time range criteria, then both clusters are declared to be in-time clusters. However, when R_{II} does not satisfy the in-time range criteria, it is unknown which cluster causes the ratio to be in the out-time ratio range and no declaration is made for either cluster at this step.

Isolated clusters are easily determined as well as nearby clusters which are in different super-blocks. Nearby clusters can also be in the same super-block. In the case of one of the clusters being in another super-block, a determination can be made for that cluster. When the other cluster (or even both clusters) is only in one super-block, the determination relies upon the pattern units or relative size of the energy deposits. The pattern units are only helpful when the cluster deposits enough energy into a pattern unit and when the clusters do not share pattern units. The determination of small energy deposits (< 100 MeV) is difficult when there are nearby clusters. Some of the small energy clusters are declared in-time clusters due to small fluctuations during the ADC digitization process.

6.5 Charged Event Selection

The detector's response to e^+e^- from data taken at the J/ψ resonance has been studied to develop a basic set of cuts for identifying inclusive J/ψ events. A Quantity, called *electron quality weight*, combines information from the many components that make the E760 detector have been used to identify electron tracks. The electron quality weight, EQW, is a likelihood ratio of an electron hypothesis to a background hypothesis for a charged track.

The EQW of each track is the product of ratios, probabilities of each hypothesis, for several detector component measured quantities. The EQW product is

$$EQW \equiv \prod_i \frac{f_i^{elec}(x_i)}{f_i^{bkgd}(x_i)}, \tag{6.5}$$

where x_i is the i^{th} detector component quantity and f_i^{elec} and f_i^{bkgd} are the probability distributions of this quantity for electrons and background, respectively. The detector component quantities used to define EQW are:

- pulse height in the H2 hodoscope as a function of polar track angle;
- pulse height in the Čerenkov counter, correcting for polar angle dependence and the different mirrors' photoelectron yields;

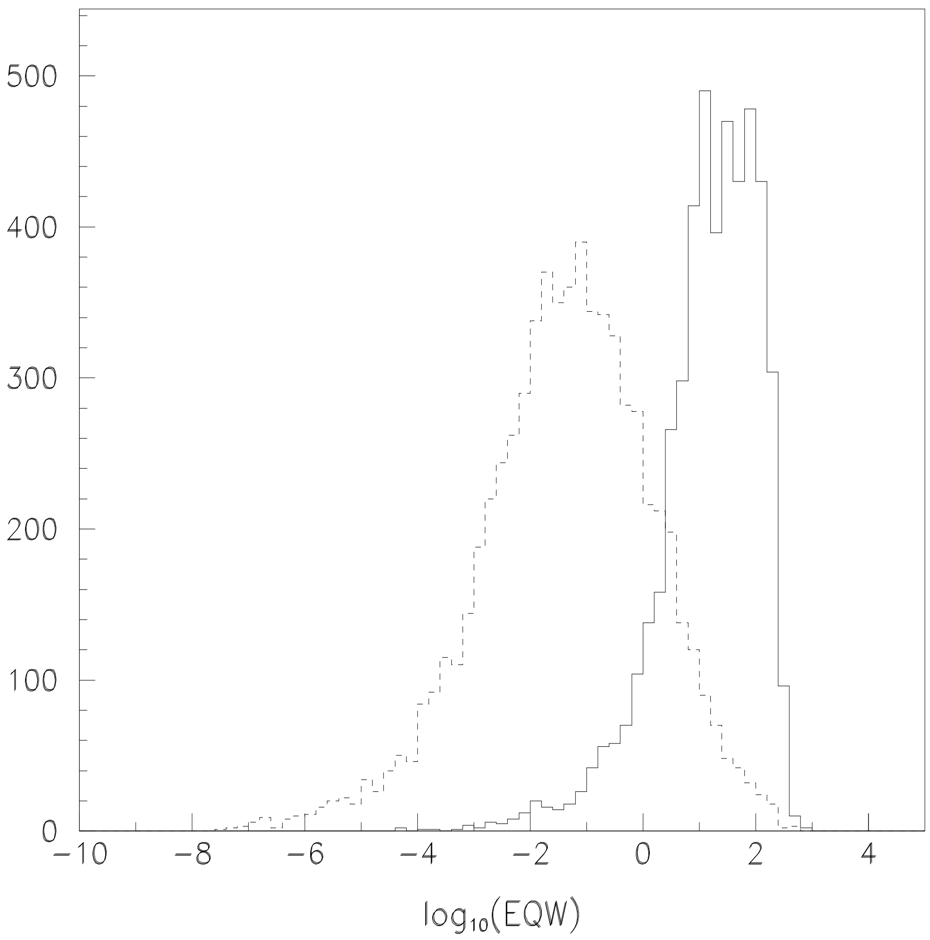

Figure 6.3: The $\log_{10} EQW$ for electrons (solid line) and background charged tracks (dashed line).

- the second moment of the central calorimeter energy deposit in the polar direction (rings);
- the second moment of the central calorimeter energy deposit in the azimuth (wedges);
- energy deposit containment in a 3×3 grid versus a 5×5 grid centered about the cluster position; and

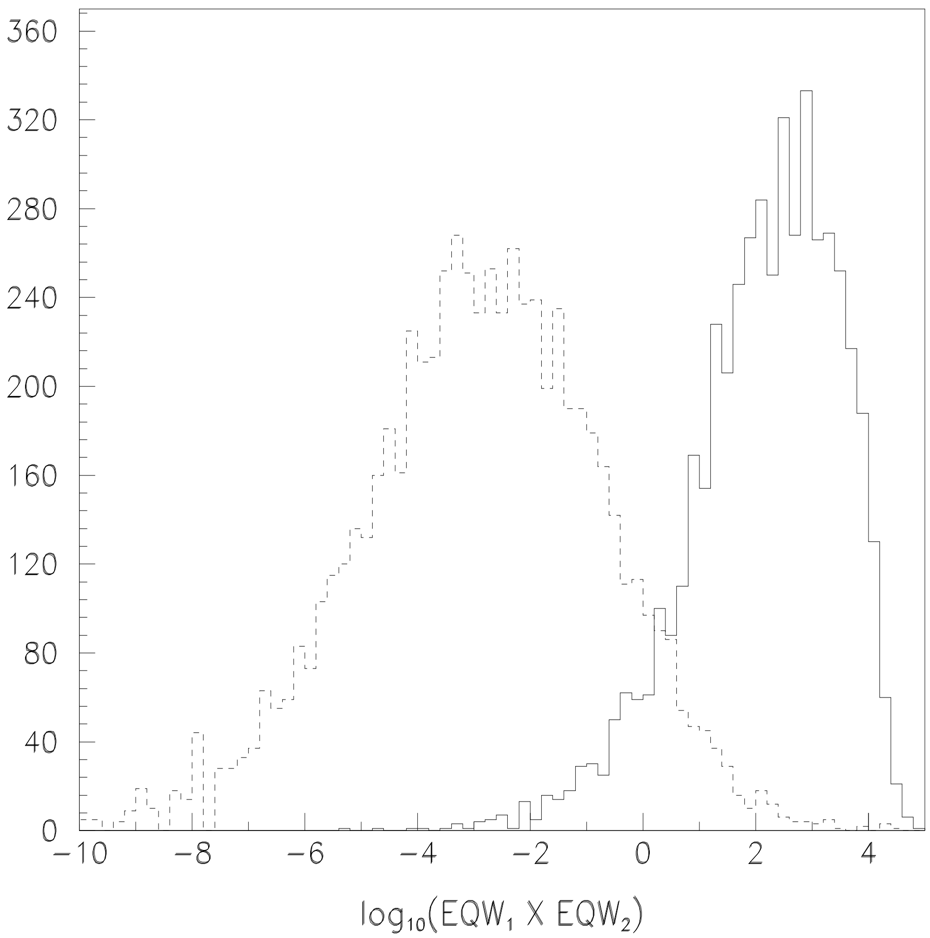

Figure 6.4: The $\log_{10}$ (product of two EQW) for e^+e^- (solid line) and background charged tracks (dashed line).

- a dE/dx measurement in the RPC, when the RPC is considered working.

The electron probability distribution for each detector component quantity is determined from studying kinematically fitted data taken at the J/ψ. Charged data taken at the $^1P_1$ are used to determine the background probability distributions. The EQW for electrons from J/ψ decays and from background charged tracks is shown in figure 6.3. The product, $EQW_1 \times EQW_2$ (the EQW's of each track), separates events with e^+e^- from the background events and is shown in figure 6.4.

6.5.1 Inclusive J/ψ Events

The inclusive selection requires the product of EQW's of the two charged tracks associated with the largest energy deposits to be consistent with e^+e^- events. A further cut on the characteristics of the energy deposit is a cluster mass cut (see equation 6.3). Events with either of the two largest energy deposits having a cluster mass $M_{cl} > 100$ MeV are eliminated to reject symmetric π^o energy deposits where one of the gamma rays has converted. This forces the e^- and e^+ to be isolated energy deposits. Both of the largest energy deposits are required to be in-time clusters.

A nominal fiducial volume cut eliminating electrons and positrons in ring 1 (backwards direction) is necessary so that all of the electromagnetic shower is contained. A fiducial cut in the forward direction is not necessary since when an electron (positron) is that far forward, the accompanying positron (electron) goes out the back of the calorimeter and also because the Čerenkov detector stops at 15° which is sufficiently far from the edge of the calorimeter. A further fiducial cut from the boundary of ring 1 and 2 (64.8°) to 62.0° is necessary due to shadowing by the backward Čerenkov cell's phototubes. Depending upon the azimuthal angle, a particle could pass through the phototube. Any charged particle that passes through a phototube's photocathode generates a signal which is generally of magnitude larger than electron tracks from the rest of the cell. Also electrons (identified kinematically at the J/ψ) in this polar region which do not pass through a Čerenkov detector phototube generally do not result in Čerenkov photoelectrons. The placement of the backward Čerenkov cells' phototubes does not make it possible to discriminate electrons at polar angles $> 62°$.

The invariant mass of the the two largest energy deposits is calculated:

$$M_{inv} = \sqrt{(E_1 + E_2)^2 - (\vec{p}_1 + \vec{p}_2)^2}, \tag{6.6}$$

where E and $\vec{p}$ are the energies and momenta of the two largest energy clusters. Since $E_i \gg m_e$, the electrons and positrons are considered massless and the invariant mass can be calculated as

$$M_{inv} = \sqrt{2E_1E_2(1 - cos\zeta)}, \tag{6.7}$$

where ζ is the opening angle between the two clusters. The events where

$$2.9\ \mathrm{GeV/c^2} > M_{inv} > 3.3\ \mathrm{GeV/c^2} \tag{6.8}$$

are considered inclusive J/ψ events.

6.5.2 Exclusive Charged Events

The exclusive event selection starts from the inclusive event selection. The exclusive J/ψ reactions are

$$\bar{p}p \to \quad J/\psi\pi^o \quad \to e^+e^-\gamma\gamma, \tag{6.9}$$

$$\bar{p}p \to \quad J/\psi\pi^o\pi^o \quad \to e^+e^-\gamma\gamma\gamma\gamma, \tag{6.10}$$

$$\bar{p}p \rightarrow \quad J/\psi\pi^+\pi^- \quad \rightarrow e^+e^-\pi^+\pi^-. \tag{6.11}$$

All final state particles are subject to the backward fiducial volume cut: $\theta_i < 62°$. The exclusive selection for each reaction (described below) includes a modified cut on the number of clusters, where the central calorimeter's cluster threshold for the central counters is 5 MeV and the threshold for the total energy deposited is 20 MeV. There are further requirements for the non-electron particles including different geometrical cuts. Events are fit by SQUAW routines to the appropriate reaction hypothesis.

The pile-up analysis is used to reject events with unassociated clusters; an unassociated cluster is defined as an in-time or a non-determined cluster with > 100 MeV energy deposited which is not associated with any of the final particles of the reaction being investigated. In addition, the forward calorimeter clusters, using the timing of its summed signals to define whether a cluster signal is from the trigger interaction or not, are treated the same as the central calorimeter clusters. No unassociated clusters are allowed for final states which do not have charged pions. In-time or non-determined clusters with energies < 100 MeV can be final state particles; otherwise these small energy clusters are ignored.

The γ's from events for reaction 6.9 and 6.10, are allowed to populate the forward calorimeter and therefore there is no forward fiducial cut. The γ's located in the central calorimeter are subject to the same invariant cluster mass cut as the e^+ and e^- clusters. The invariant mass of a $\gamma\gamma$ pair, $M_{\gamma\gamma} = M_{inv}$ (equation 6.7) must be near the π^o mass,

$$50 \text{ MeV/c}^2 < M_{\pi^o} < 200 \text{ MeV/c}^2. \tag{6.12}$$

The $J/\psi\pi^o$ candidate events are subject to a 6C fit. A 7C fit is done to the $J/\psi\pi^o\pi^o$ candidate events.

For reaction 6.11, both the π^+ and π^- are required to have good charged tracks and are therefore subject to a geometrical cut of $\theta > 15°$. The modified cluster cut is relaxed since a charged pion signal in the central calorimeter may be large and/or asymmetric (and therefore can be split into two clusters) and also the low energy charged pions do not necessarily generate a central calorimeter signal . The unassociated cluster cut is only applied when an extra energy deposit (> 100 MeV) is not associated with one of the four charged tracks. The pions are required to be well separated in the azimuth from the e^+e^- tracks by requiring that the four charged particles hit different H2 elements. Since a charged track can cause signals in two neighboring H2 elements, the requirement is that tracks can not be from contiguous H2 elements. A 3C fit is performed on possible $J/\psi\pi^+\pi^-$candidate events.

6.6 Neutral Event Selection

The search for radiative decays of the $^1\text{P}_1$ to η_c (reaction 1.2) begins with the neutral DSTs. The η_c is identified by either decaying to $\gamma\gamma$ (reaction 1.4) or to three neutral mesons (π^o, η and/or η') which all subsequently decay into pairs of gamma rays. The search for the all neutral channels involves either a 3γ or 7γ final state.

The energy of the transition gamma ray is ≈ 545 MeV which is approximately the average energy of the gamma rays in the center of mass for the 7γ final state.

Since no pile-up information for the forward calorimeter is included in the neutral DSTs, a forward as well as backward fiducial cut is made; no clusters are allowed in the forward calorimeter. All gamma rays are required to be away from the edges of the central calorimeter, $13° < \theta_\gamma < 62°$. Any cluster that is associated with a γ is expected to have a cluster mass < 100 MeV. The cluster mass is used to reject symmetric π^o energy deposits.

The number of clusters, on-time or non-determined, must equal exactly the number of final state particles, i.e., no extra in-time or non-determined clusters of any energy (> 25 MeV) are allowed. The 3γ and 7γ final states are permitted to have different minimum energies for the gamma rays: 100 MeV and 50 MeV, respectively. Other cuts which are different, depending upon the final state, are described below.

Background for the 3γ final state comes from π^o's and η's. Events are rejected whenever one of the three two-cluster invariant masses is near one of these masses: equation 6.12 and

$$400 \text{ MeV/c}^2 < M_\eta < 700 \text{ MeV/c}^2. \tag{6.13}$$

An event is kept when one of the invariant mass combinations is near the η_c mass:

$$2.7 \text{ GeV/c}^2 < M_{\eta_c} < 3.2 \text{ GeV/c}^2. \tag{6.14}$$

The events which pass the invariant mass requirements are then fit ($5C$) by the SQUAW routines.

The large number of 7 cluster neutral events and the many possible orderings of the gamma rays has led to applying several criteria before attempting a fit of an event. The total longitudinal and transverse lab momenta of the gamma rays have the requirements:

$$5.0 \text{ GeV/c} < \sum_{i=1}^{7} P_{\|_i} < 6.2 \text{ GeV/c} \tag{6.15}$$

and

$$\sum_{i=1}^{7} P_{\perp_i} < 200 \text{ MeV/c}. \tag{6.16}$$

All combinations of pairs of gamma rays are tried. An acceptable order occurs when one gamma ray's measured energy is within 50% of the expected transition energy and the other six gamma rays are paired to make three neutral mesons. The invariant mass of a pair is accepted when it is near the π^o mass (equation 6.12), η mass (equation 6.13), or η' mass:

$$750 \text{ MeV/c}^2 < M_{\eta'} < 1150 \text{ MeV/c}^2. \tag{6.17}$$

A combination is fit ($8C$) by SQUAW routines to one of the following reactions:

$$\bar{p}p \rightarrow {}^1\text{P}_1 \rightarrow \gamma\eta_c \rightarrow \quad \gamma\pi^o\pi^o\pi^o \tag{6.18}$$

$$\gamma\pi^o\pi^o\eta \tag{6.19}$$

$$\gamma\pi^o\pi^o\eta' \tag{6.20}$$

$$\gamma\pi^o\eta\eta \tag{6.21}$$

$$\gamma\pi^o\eta\eta' \tag{6.22}$$

$$\gamma\pi^o\eta'\eta' \tag{6.23}$$

$$\gamma\eta\eta\eta \tag{6.24}$$

$$\gamma\eta\eta\eta' \tag{6.25}$$

$$\gamma\eta\eta'\eta' \tag{6.26}$$

$$\gamma\eta'\eta'\eta' \quad \rightarrow 7\gamma. \tag{6.27}$$

The η_c has been observed to decay [21] into $\pi^o\pi^o\eta$ and $\pi^o\pi^o\eta'$ (reactions 6.19 and 6.20); decays involving 1 or 3 π^o's are isospin violating (reactions 6.18 and 6.21 to 6.23). Furthermore, the hypotheses

$$\bar{p}p \rightarrow {}^1\mathrm{P}_1 \rightarrow \quad \gamma\eta' \rightarrow \gamma\pi^o\pi^o\pi^o \tag{6.28}$$

$$\gamma\eta' \rightarrow \gamma\pi^o\pi^o\eta \tag{6.29}$$

$$\gamma\eta \rightarrow \gamma\pi^o\pi^o\pi^o \quad \rightarrow 7\gamma, \tag{6.30}$$

are also tried when the transition gamma ray energy matches the appropriate hypothesis. All combinations are tried and the largest χ^2 fit probabilities for reactions 6.18 to 6.30 are kept for each event.

If any of the χ^2 fit probabilities is $> 1\%$ for an event, then two different sets of possible background reactions are tried using the same meson mass windows (equations 6.12, 6.13 and 6.17) for all possible combinations. The first set assumes 4 neutral mesons decaying to 8γ where one gamma ray is not detected. The possible ($5C$) fits to the following hypotheses are performed:

$$\bar{p}p \rightarrow \quad \pi^o\pi^o\pi^o\pi^o \tag{6.31}$$

$$\pi^o\pi^o\pi^o\eta \tag{6.32}$$

$$\pi^o\pi^o\pi^o\eta' \tag{6.33}$$

$$\pi^o\pi^o\eta\eta \tag{6.34}$$

$$\pi^o\pi^o\eta\eta' \tag{6.35}$$

$$\pi^o\pi^o\eta'\eta' \tag{6.36}$$

$$\pi^o\eta\eta\eta \tag{6.37}$$

$$\pi^o\eta\eta\eta' \tag{6.38}$$

$$\pi^o\eta\eta'\eta' \tag{6.39}$$

$$\pi^o\eta'\eta'\eta' \tag{6.40}$$

$$\eta\eta\eta\eta \tag{6.41}$$

$$\eta\eta\eta\eta' \tag{6.42}$$

$$\eta\eta\eta'\eta'. \tag{6.43}$$

The second set of hypotheses is two neutral mesons plus ω, with ω decaying to $\pi^o\gamma$, resulting in 7γ. Combinations are fit ($8C$) to the following possible background reactions:

$$\bar{p}p \rightarrow \quad \pi^o\pi^o\omega \tag{6.44}$$

$$\pi^o\eta\omega \tag{6.45}$$

$$\pi^o\eta'\omega \tag{6.46}$$

$$\eta\eta\omega \tag{6.47}$$

$$\eta\eta'\omega \tag{6.48}$$

$$\eta'\eta'\omega. \tag{6.49}$$

The largest χ^2 fit probabilities for all 7γ possible final states (reactions 6.18 to 6.30) and background reactions (reactions 6.31 to 6.49) are kept and compared. An event is assigned to the hypothesis with the largest χ^2 fit probability.